Comparison of the Membrane Association of Two Antimicrobial Peptides, Magainin 2 and Indolicidin

Hongxia Zhao, Juha-Pekka Mattila, Juha M. Holopainen, and Paavo K. J. Kinnunen
Helsinki Biophysics and Biomembrane Group, Institute of Biomedicine, University of Helsinki, FIN-00014 Helsinki, Finland

ABSTRACT Interactions of two antimicrobial peptides, magainin 2 and indolicidin, with three different model biomembranes, namely, monolayers, large unilamellar vesicles (LUVs), and giant liposomes, were studied. Insertion of both peptides into lipid monolayers was progressively enhanced when the content of an acidic phospholipid, 1-palmitoyl-2-oleoyl-*sn*-glycero-3-phosphoglycerol (POPG) in a film of 1-stearoyl-2-oleoyl-*sn*-glycero-3-phosphocholine (SOPC) was increased. Indolicidin and magainin 2 penetrated also into lipid monolayers containing cholesterol (mole fraction, $X = 0.1$). Membrane association of magainin 2 attenuated lipid lateral diffusion in POPG-containing LUVs as revealed by the decrease in the excimer/monomer fluorescence ratio I_e/I_m for the pyrene fatty-acid-containing phospholipid derivative 1-palmitoyl-2-[10-(pyren-1-yl) decanoyl]-*sn*-glycero-3-phospho-*rac*-glycerol (PPDPG). Likewise, an increase in steady-state fluorescence anisotropy of the membrane-incorporated diphenylhexatriene (DPH) was observed, revealing magainin 2 to increase acyl chain order and induce segregation of acidic phospholipids. Similar effects were observed for indolicidin. The topological effects of magainin 2 and indolicidin on phospholipid membranes were investigated using optical microscopy of giant vesicles. Magainin 2 had essentially no influence on either SOPC or SOPC:cholesterol ($X = 0.1$) giant liposomes. However, effective vesiculation was observed when acidic phospholipid ($X_{PG} = 0.1$) was included in the giant vesicles. Indolicidin caused only a minor shrinkage of giant SOPC vesicles whereas the formation of endocytotic vesicles was observed when the giant liposome contained POPG ($X_{PG} = 0.1$). Interestingly, for indolicidin, vesiculation was also observed for giant vesicles composed of SOPC/cholesterol ($X_{chol} = 0.1$). Possible mechanisms of membrane transformation induced by these two peptides are discussed.

INTRODUCTION

During the last decade an increasing number of antimicrobial peptides, such as cecropins, defensins, magainins, melittin, indolicidin, and alamethicin, have been discovered in animals and plants as well as bacteria. These peptides serve in the vertebrates and invertebrates for both offensive and defensive purposes (Sansom, 1991; Saberwal and Nagaraj, 1994; Matsuzaki, 1998) by interacting with the lipids and somehow disturbing the barrier properties of the membranes of the target cells (Bechinger, 1997; Matsuzaki, 1998, 1999; Oren and Shai, 1998; Shai, 1999; Sitaram and Nagaraj, 1999). Being cationic, antimicrobial peptides interact preferentially with acidic lipids, which are particularly abundant in bacteria (Op den Kamp, 1979), thus providing the basis for differences in cell specificity (Matsuzaki et al., 1995a). The above characteristics make these peptides an interesting area for studies on lipid-protein interactions and may further allow for developing novel antimicrobial, anticancer, and antiviral compounds.

We report here on a comparison of the interactions with lipid membranes of two antimicrobial peptides, magainin 2 and indolicidin. Magainin and indolicidin belong to different antimicrobial peptide families classified by their amino acid composition and secondary structure (Falla et al., 1996). Accordingly, magainin is a paradigm of the group that assumes an amphipathic α-helical structure in lipid membranes (Matsuzaki, 1999), whereas indolicidin belongs to another group with a unique amino acid composition and a non-α-helical conformation in lipid bilayers (Ladokhin et al., 1999; Ha et al., 2000). Magainins were discovered in the skin of the African clawed frog *Xenopus laevis* and show a broad spectrum of antimicrobial (Zasloff, 1987; Zasloff et al., 1988) and anticancer cell activities (Cruciani et al., 1991; Baker et al., 1993) at nonhemolytic concentrations. To this end, it is of interest that extracts of frog skin have been used in traditional Chinese medicine for the control of skin infections (L. Miao, University of Roskilde, personal communication, 2000). Magainin 2 consists of 23 amino acid residues (GIGKFLHSAKKFGKAFVGEIMNS), has a positive net charge of +4, and exerts its antimicrobial activity by permeabilizing the bacterial membrane (Matsuzaki et al., 1997). It has been proposed that a peptide-lipid supramolecular complex pore is formed, allowing for transbilayer traffic of ions, lipids, and peptides, with simultaneous dissipation of transmembrane potential and lipid asymmetry (Matsuzaki et al., 1995a,b,c, 1996, 1998; Ludtke et al., 1996). Spectroscopic and kinetic studies on the effects of magainin on submicroscopic lipid vesicles (Matsuzaki et al., 1995a,b,c, 1996, 1998; Ludtke et al., 1996) have revealed the cooperative nature of the interactions. However, the exact mechanisms of membrane perturbation by magainin remain controversial.

Indolicidin is found in cytoplasmic granules of bovine neutrophils (Selsted et al., 1992) and has a unique amino acid composition with five Trp and three Pro residues in its

Received for publication 8 January 2001 and in final form 11 July 2001.
Address reprint requests to Dr. Paavo K. J. Kinnunen, Helsinki Biophysics and Biomembrane Group, Institute of Biomedicine, P.O. Box 63 (Haartmaninkatu 8), FIN-00014 University of Helsinki, Finland. Tel.: 358-9-19125400; Fax: 358-9-19125444; E-mail: Paavo.Kinnunen@Helsinki.Fi.

0006-3495/01/11/2979/13 $2.00

13-amino-acid sequence (ILPWKWPWWPWRR). It is one of the shortest natural linear antimicrobial peptides and, similarly to magainin, has activity against both Gram-negative and -positive bacteria (Selsted et al., 1992) and fungi (Ahmad et al., 1995) as well as protozoa (Aley et al., 1994). Indolicidin is cytotoxic also to rat and human T lymphocytes (Schluesener et al., 1993), lyses red blood cells (Ahmad et al., 1995), and has activity against HIV-1 (Robinson et al., 1998). Indolicidin preferentially binds to acidic phospholipid, although it also associates with neutral phospholipids (Ladokhin et al., 1997). Indolicidin has been shown to permeabilize the outer membrane of *Escherichia coli* (Falla et al., 1996; Subbalakshmi et al., 1996) to form channels as revealed by conductance measurements with planar bilayers (Falla et al., 1996; Wu et al., 1999). Indolicidin's high affinity to membranes, unusual amino acid composition, and small size make it an intriguing antimicrobial agent. Its antimicrobial activity, the charge requirement, and also the importance of Trp and Pro residues for biological activity have been extensively studied (Sitaram and Nagaraj, 1999). However, the molecular mechanisms underlying peptide-mediated cell lysis, i.e., whether the peptide forms pores, dissolves the membranes like a detergent, or induces membrane defects, remain matters of debate (Sitaram and Nagaraj, 1999).

Small and large unilamellar vesicles (LUVs) continue to be widely exploited as model membranes. However, these liposomes are submicroscopic and do not allow resolution of morphological features relevant to more macroscopic changes in biomembranes. The so-called giant vesicles (10–500 μm), which are spherical, closed molecular bilayers and entrap an aqueous compartment, are instead good models for studies of undulation, budding, wounding, healing, and other manifestations of cell-like behavior induced by membrane-acting reagents (Riquelme et al., 1990; Menger, 1998; Menger and Lee, 1995; Menger and Keiper, 1998; Angelova and Tsoneva, 1999; Angelova et al., 1999; Holopainen et al., 2000). Due to their large size, giant vesicles can be observed by light microscopy, permitting direct visualization of processes involving supramolecular chemistry and biophysics (Luisi and Walde, 2000). In this study, we used different membrane models, namely, monolayers, large unilamellar vesicles, and giant liposomes, respectively, to investigate the penetration of magainin and indolicidin into films, their effects on the dynamics of lipids in bilayers, and macroscopic, morphological changes in membranes.

MATERIALS AND METHODS

Materials

Hepes, EDTA, and magainin 2 were from Sigma (St. Louis, MO) and indolicidin from Bachem (Bubendorf, Switzerland). The purity of the peptides were >99% and >95%, respectively, as verified by high-performance liquid chromatography analysis provided by their respective suppliers. The correct molecular weights and purity of magainin 2 and indolicidin were confirmed by mass spectroscopy. 1-Stearoyl-2-oleoyl-*sn*-glycero-3-phosphocholine (SOPC), 1-palmitoyl-2-oleoyl-*sn*-glycero-3-phosphoglycerol (POPG), and β-cholesterol were from Avanti Polar Lipids (Alabaster, AL). For the fluorescent phospholipid analogs, 1-palmitoyl-2-[10-(pyren-1-yl)decanoyl]-*sn*-glycero-3-phospho-*rac*-glycerol (PPDPG) and 1-palmitoyl-2-[10-(pyren-1-yl)decanoyl]-*sn*-glycero-3-phosphocholine (PPDPC) were from K&V Bioware (Espoo, Finland). Diphenylhexatriene (DPH) was from EGA Chemie (Steinheim, Germany). Concentrations of the nonlabeled lipids were determined gravimetrically with a high-precision electrobalance (Cahn, Cerritos, CA) and those of the pyrene-containing phospholipids and DPH spectrophotometrically, by absorbance at 341 nm, using molar extinction coefficients of 38,000 cm^{-1} and 88,000 cm^{-1}, respectively. The purity of the lipids was checked by thin layer chromatography on silicic-acid coated plates (Merck, Darmstadt, Germany) developed with chloroform/methanol/water (65:25:4, v/v/v). Examination of the plates after iodine staining and, when appropriate, upon UV illumination revealed no impurities.

Penetration of the peptides into lipid monolayers

Penetration of peptides into monomolecular lipid films was measured using magnetically stirred circular Teflon wells (Multiwell plate, subphase volume 1.2 ml, Kibron, Helsinki, Finland). Surface pressure (π) was monitored with a Wilhelmy wire attached to a microbalance (Delta Pi, Kibron) connected to a Pentium PC. Lipids were mixed in the indicated molar ratios in chloroform (~1 mg/ml) and then spread in this solvent onto the air-buffer (5 mM Hepes, 0.1 mM EDTA, pH 7.0) interface. Subsequently, the lipid monolayers were allowed to equilibrate for ~15 min at different initial surface pressures (π_0) before the injection of magainin 2 or indolicidin into the subphase. The final concentration of the peptides was 1 μM. The increments in π after the injection of peptides were complete in ~30 min, and the difference between the initial surface pressure (π_0) and the value observed after the penetration of peptides into the films was taken as $\Delta\pi$. The data shown represent averages from triplicate measurements and are represented as $\Delta\pi$ versus π_0. All measurements were performed at ambient temperature (~24°C).

Preparation of LUVs

The indicated lipids were mixed in chloroform after which the solvents were removed under a stream of nitrogen and the lipid residue subsequently maintained under reduced pressure for at least 2 h. The dry lipids were then hydrated at 50°C to yield a lipid concentration of 1 mM. The resulting dispersions were extruded through a stack of two polycarbonate filters (100-nm pore size, Millipore, Bedford, MA) using a Liposofast-low-pressure homogenizer (Avestin, Ottawa, Canada) to obtain LUVs.

Measurement of I_e/I_m

Pyrene is a paradigm for excimer-forming organic fluorophores, and its derivatives are widely exploited in studies on biomolecules. A monomeric pyrene emits fluorescence with a wavelength at ~398 nm, and the excimer (excited dimer) relaxes back to two ground-state pyrenes by emission with a maximum at ~480 nm. Steady-state I_e/I_m values provide a reasonably good measure of qualitative changes in the collision frequency of the probes, mirroring both lateral diffusion and local concentration of the pyrene-labeled lipids (for brief reviews, see Kinnunen et al., 1993; Duportail and Lianos, 1996). Fluorescence emission spectra for LUVs labeled with PPDPG or PPDPC ($X = 0.01$) were measured with a Perkin-Elmer LS50B spectrofluorometer with a magnetically stirred, thermostatted cuvette compartment using excitation wavelength of 344 nm. Bandwidths of 5 nm were used for both excitation and emission. The lipid concentration used was 25 μM with temperature maintained at 25°C. After addition of

appropriate amounts of peptides, samples were equilibrated for 5 min before recording the spectra. Three scans were averaged, and the emission intensities at ~398 and 480 nm were taken for I_m and I_e, respectively. All measurements were repeated three times.

Fluorescence anisotropy of DPH

DPH was included into liposomes at $X = 0.002$. The lipid concentration used was 25 μM with temperature maintained at 25°C. Polarized emission was measured in L-format using Polaroid-type filters with Perkin-Elmer LS50B. Fluorescence anisotropy r for DPH was measured with excitation at 360 nm and emission at 450 nm, using 5=nm bandwidths, and its values were calculated using routines of the software provided by Perkin-Elmer. All measurements were repeated three times.

Formation of giant liposomes

Giant liposomes were prepared as described elsewhere (Angelova and Dimitrov, 1986; Holopainen et al., 2000). Briefly, ~1–3 μl of the desired lipids dissolved in diethylether:methanol (9:1, v/v, final total lipid concentration 1 mM) were spread on the surface of two Pt electrodes and subsequently dried under a stream of nitrogen. Possible residues of organic solvent were removed by evacuation in vacuum for 1 h. A glass chamber with the attached electrodes and a quartz window bottom was placed on the stage of a Zeiss IM-35 inverted fluorescence microscope. An AC field (sinusoidal wave function with a frequency of 4 Hz and an amplitude of 0.2 V) was applied before adding 1.3 ml of 0.5 mM Hepes buffer, pH 7.4. During the first minute of hydration the voltage was increased to 1.0–1.2 V. The AC field was turned off after 2–4 h, and giant liposomes were observed with Hoffman modulation contrast (HMC) optics with a 10×/0.25 objective (Modulation Optics, New York, NY). The size of giant liposomes was measured using calibration of the images by motions of the micropipette as proper multiples of the step length (50 nm) of the micromanipulator (MX831 with MC2000 controller, SD Instruments, Grants Pass, Oregon). Images were recorded with a Peltier-cooled 12-bit digital CCD camera (C4742–95, Hamamatsu, Hamamatsu City, Japan) interfaced to a computer and operated by the software (HiPic 5.0.1) provided by the manufacturer.

Microinjection techniques

Micropipettes with inner tip diameters of >0.5 μm (Schnorf et al., 1994) were made from borosilicate capillaries (1.2-mm outer diameter) by a microprocessor-controlled horizontal puller (P-87, Sutter Instrument Co., Novato, CA). Indicated amounts of the peptide solutions (0.5 mM in 10 mM Hepes, 0.1 mM EDTA, pH 7.0) were applied onto the outer surface of individual giant vesicles as a series of single injections of ~20 fl delivered with a pneumatic microinjector (PLI-100, Medical Systems Corp., Greenvale, NY). For easier handling only vesicles attached to the electrode surface were used. All experiments were performed at ambient temperature (~24°C) and were repeated at least 10 times.

RESULTS

Penetration of the antimicrobial peptides into lipid monolayers

The intercalation of the antimicrobial peptides into lipid monolayers spread at the air/water interface to different initial surface pressures (π_0) was observed by measuring the increment in surface pressure ($\Delta\pi$) following the addition of the peptides into the subphase (Brockman, 1999; Verger and Pattus, 1976). Magainin 2 readily inserted into SOPC monolayers at $\pi_0 > 12$ mN/m (Fig. 1 *A*), whereas above $\pi_0 \approx 35$ mN/m its penetration into the film was abolished, this value thus representing the critical packing pressure π_c for the interaction of this peptide with SOPC films. In keeping with its net positive charge of +4 (Matsuzaki, 1998), the penetration of magainin 2 into the lipid monolayer was progressively augmented when the content of the acidic phospholipid POPG in the film was increased (Fig. 1 *A*). Accordingly, the values for π_c abrogating the intercalation of magainin 2 into the monolayer were increased to ~39 ($X_{PG} = 0.1$), 43 ($X_{PG} = 0.2$), and 46 mN/m ($X_{PG} = 0.4$) (Fig. 1 *C*). Instead, the inclusion of cholesterol ($X_{chol} = 0.1$) into the SOPC film had no significant effect on the penetration of magainin 2 (Fig. 1 *A*).

A pronounced increase in π was observed also for indolicidin, revealing its insertion into the SOPC monolayers (Fig. 1 *B*). However, indolicidin is significantly more membrane active than magainin 2, with $\pi_c \approx 65$mN/m for a film of SOPC. Similarly to magainin 2, the presence of increasing contents of POPG in the monolayer enhanced the penetration of indolicidin, increasing $\Delta\pi$ below ~38 mN/m, and in keeping with an electrostatic interaction between the peptide and the lipid monolayer. However, above the latter value for surface pressure the increment in π due to indolicidin was attenuated by POPG. Thus, in contrast to magainin 2, there was now a decrement in π_c in the presence of POPG (Fig. 1 *C*), shifting from ~65 mN/m (for a SOPC monolayer) to ~50 mN/m at $X_{PG} = 0.4$. The increment in π by indolicidin was augmented also by cholesterol ($X = 0.1$) in a SOPC monolayer, whereas π_c decreased to ~54 mN/m. The patterns evident in Fig. 1 for magainin 2 and indolicidin are very different, with a distinct crossover point at ~38 mN/m for the latter peptide.

Effects of the antimicrobial peptides on the lipid dynamics in bilayers

Subsequently to the above monolayer studies it was of interest to explore the impact of the peptides on lipid dynamics. This was accomplished using fluorescence spectroscopy and LUVs of varying lipid compositions, recording emission spectra for the pyrene-labeled fluorescent phospholipid analogs PPDPC or PPDPG (both at $X = 0.01$). For SOPC LUVs the addition of magainin 2 caused significant quenching of pyrene fluorescence, the intensities of both pyrene monomer and excimer emission decreasing in parallel, as shown for I_m (Fig. 2). Consequences of the association of magainin 2 with liposomes were studied also as a function of X_{PG}. Upon increasing X_{PG} from 0.1 to 0.4, progressively enhanced I_m at 398 nm (RFI_m) due to magainin 2 was observed whereas the initial increment in I_m leveled off at well defined PG/magainin 2 stoichiometries of ~2, 3, and 5 (Fig. 2 *A*). Following this initial phase up to the given stoichiometries there was a second process, the slope

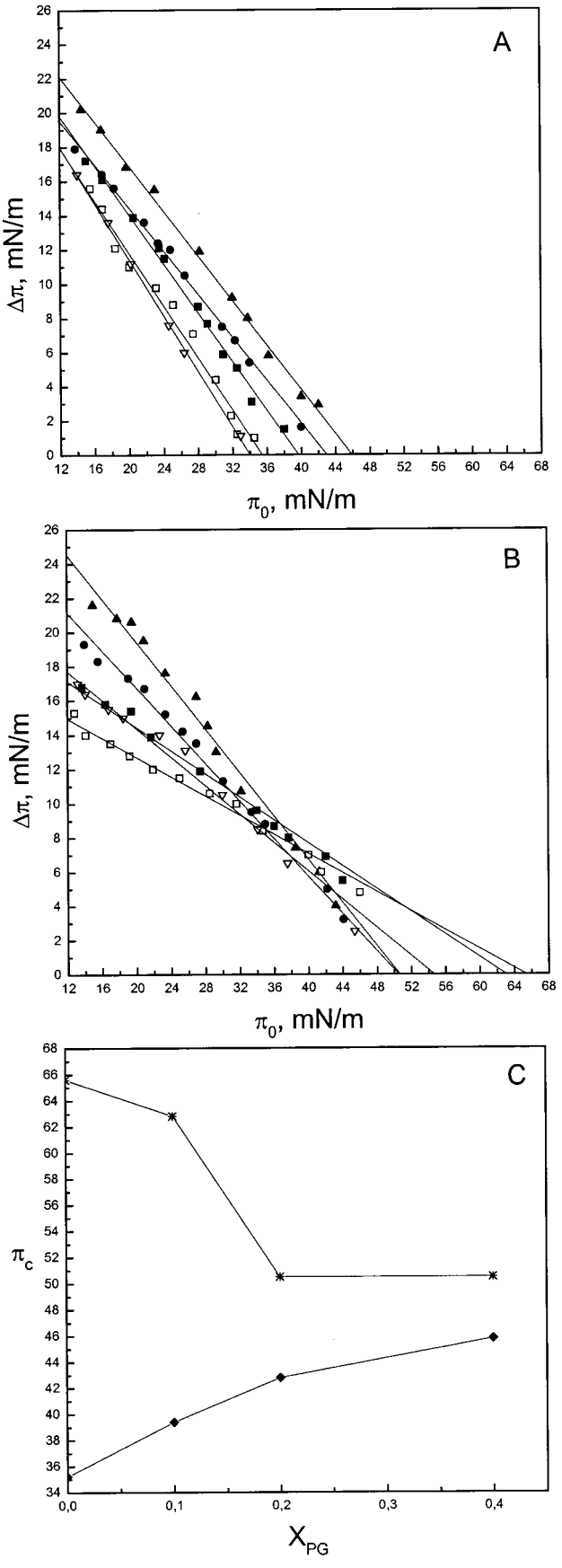

of which also increased with X_{PG} (Fig. 2 *B*). Magainin 2 caused only insignificant changes in I_e/I_m at $X_{PG} = 0$ and 0.1, whereas at $X_{PG} = 0.2$ and 0.4, decrements by 10% and 25%, respectively, were evident (Fig. 3 *A*). To distinguish between two qualitatively different changes in lipid dynamics, namely, lateral mobility and microdomain formation, as underlying causes for the above changes in I_e/I_m we also assessed changes in acyl chain order by measuring fluorescence anisotropy r for DPH (Fig. 3 *B*). Magainin 2 caused virtually no changes in r in the absence of the acidic phospholipid (Fig. 3 *B*). However, progressively augmented lipid packing and acyl chain order upon the addition of magainin 2 were evident with increasing X_{PG} (Fig. 3 *B*), with maximally 1.4-fold increment in r at $X_{PG} = 0.4$. Notably, lack of changes in I_e/I_m at $X_{PG} = 0.1$ together with the increase in acyl chain order reveal that microscopic enrichment of PPDPG is taking place. Interestingly, in the presence of cholesterol ($X_{chol} = 0.1$), both I_m and I_e decreased dramatically due to magainin 2, with insignificant changes in I_e/I_m (Figs. 2 *A* and 3 *A*). Enhanced membrane order by the incorporation of cholesterol in the membrane is revealed by the increase in r before the addition of the peptide (Fig. 3 *B*), as reported previously (van Ginkel et al., 1989). However, magainin 2 had no further effect on r in the presence of cholesterol ($X_{chol} = 0.1$, Fig. 3 *B*).

Subsequently, we carried out identical measurements as above but using indolicidin. Similarly to magainin 2, indolicidin also caused a parallel decrease in both I_m and I_e for SOPC LUVs, illustrated here for I_m (Fig. 4 *A*). However, in contrast to magainin 2, quenching of pyrene fluorescence was evident also when the acidic phospholipid POPG was present. When the peptide/lipid molar ratio was $<1/20$, I_m decreased in the sequence $X_{PG} = 0.4 < 0.2 < 0.1 < 0$. At $X_{PG} = 0.4$ and upon peptide/lipid molar ratio $>1{:}12.5$ the values for I_m decreased further. The maximal decrement in I_m due to indolicidin was from 15% (at $X_{PG} = 0$) to 40% (at $X_{PG} = 0.4$). Despite the decrease in I_m, I_e/I_m revealed no significant changes due to indolicidin (Fig. 4 *B*). Interestingly, the largest decrease in I_m was measured at $X_{chol} = 0.1$ (Fig. 4 *A*). Similarly to magainin 2, DPH anisotropy r remained constant when indolicidin was added to SOPC LUVs (Fig. 5 *A*). However, augmented lipid packing and increased acyl chain order were caused by indolicidin in

FIGURE 1 Penetration of antimicrobial peptides into lipid monolayers. Increments in surface pressure ($\Delta\pi$) of lipid monolayers due to the addition of 1 μM magainin (*A*) or indolicidin (*B*) into the subphase are illustrated as a function of the initial surface pressure (π_0). Content of the acidic POPG (X_{PG}) in SOPC was 0 (□), 0.1 (■), 0.2 (●), and 0.4 (▲). Also shown is the insertion of the peptides into a SOPC film with $X_{chol} = 0.1$ (▼). The changes of π_c as a function of X_{PG} upon the penetration of magainin (◆) and indolicidin (*) are shown in *C*. Each data point represents the mean of triplicate measurements. The standard deviation varied between 0.1 mN/m and 0.8 mN/m and for the sake of clarity is not shown.

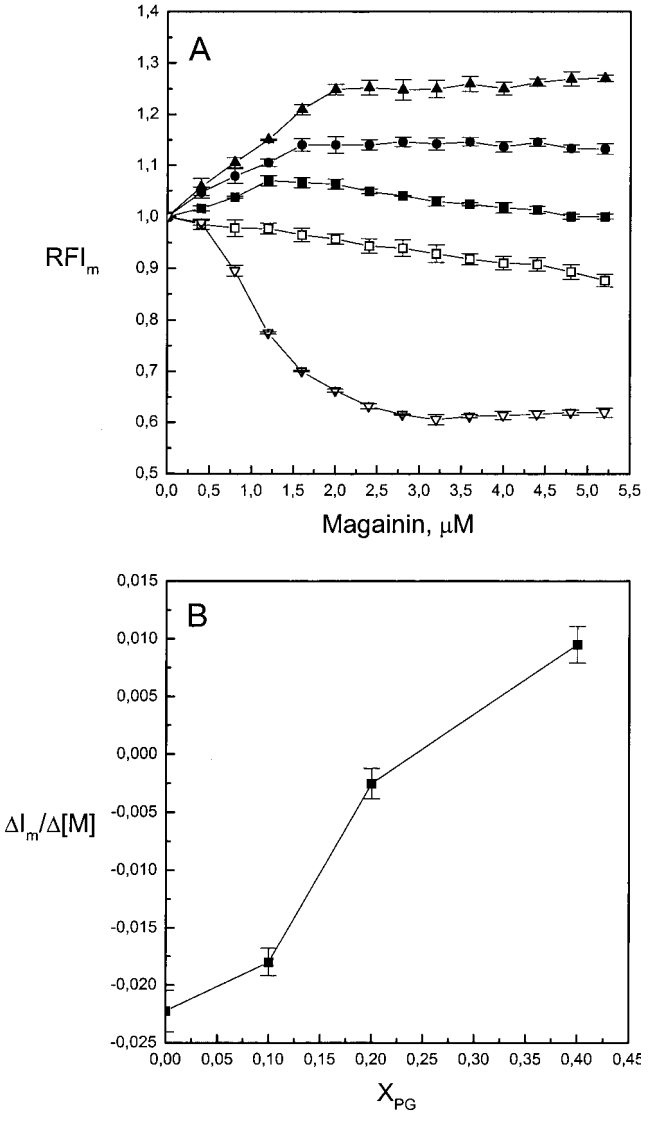

FIGURE 2 Effects of magainin on lipid dynamics in LUVs assessed by fluorescence of pyrene-labeled phospholipid analogs (X = 0.01), shown as changes in pyrene monomer emission intensity $I_m \approx 398$ nm (A) and slopes for the increase in I_m after reaching saturation response in RFI_m (B). PPDPC was used in SOPC and SOPC/cholesterol LUVs, and PPDPG in LUVs containing POPG. Liposomes were composed of SOPC with X_{PG} = 0 (□), 0.1 (■), 0.2 (●), and 0.4 (▲), and with X_{chol} = 0.1 (▼). The concentration of lipids was 25 μM in a total volume of 2 ml of 5 mM Hepes, 0.1 mM EDTA, pH 7.0. The temperature was maintained at 25°C with a circulating waterbath. Each data point represents the mean of triplicate measurements, with the error bars indicating ±SD.

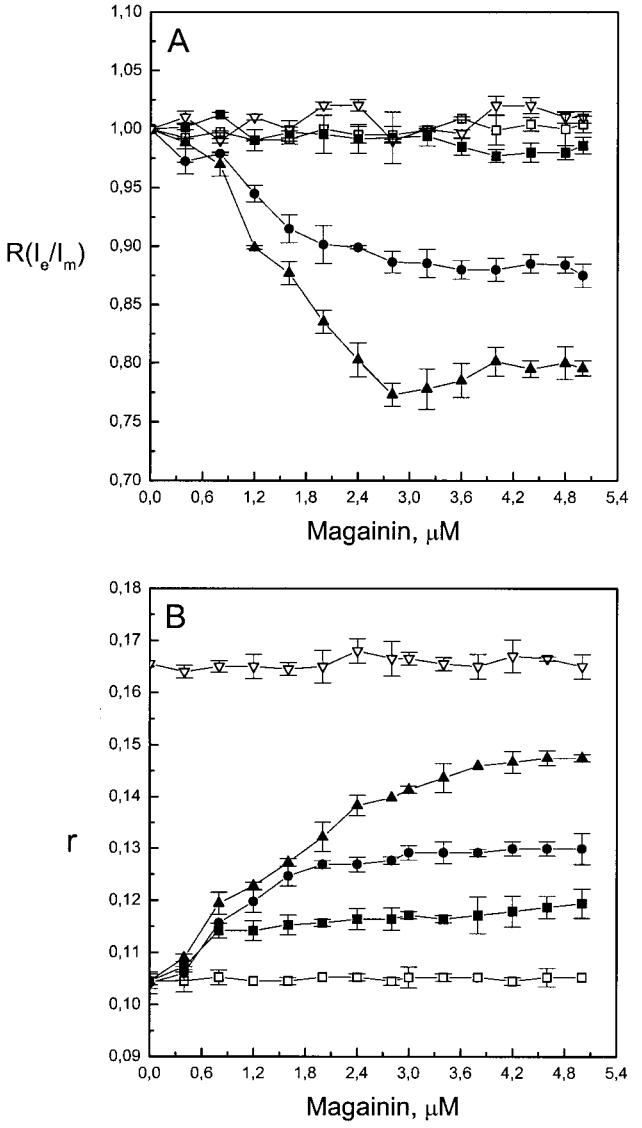

FIGURE 3 Effects of magainin on excimer to monomer ratio $R(I_e/I_m)$ of pyrene-labeled phospholipid analogs (A) and on the steady-state emission anisotropy r of DPH (X = 0.002) (B) in SOPC liposomes with X_{PG} = 0 (□), 0.1 (■), 0.2 (●), and 0.4 (▲) and with X_{chol} = 0.1 (▼). Otherwise, conditions were as described in the legend for Fig. 2.

acidic-phospholipid-containing membranes, evident as an increase in r (Fig. 5 A). Moreover, the increase in r depended on X_{PG}, increasing with the content of the acidic phospholipid in bilayers (Fig. 5 B). The corresponding maximal increase was from 1.05- to 1.39-fold. The increment in the membrane acyl chain order due to indolicidin was observed also in the presence of cholesterol, increasing r by 1.06-fold (Fig. 5 A).

Effects of antimicrobial peptides on membrane topology

Because of the pronounced and lipid-composition-dependent effects of magainin 2 and indolicidin on monolayers and LUVs described above it was of interest to compare the impact of these peptides on the three-dimensional topology of macroscopic membranes using giant liposomes, both with and without PG. Giant liposomes composed of SOPC readily formed in an AC field. SOPC membranes were unaffected by magainin 2 even when exposed to high amounts of the peptide (~2 fmol, ~4 pl = 200 repeated injections, data not shown). Likewise, also giant liposomes

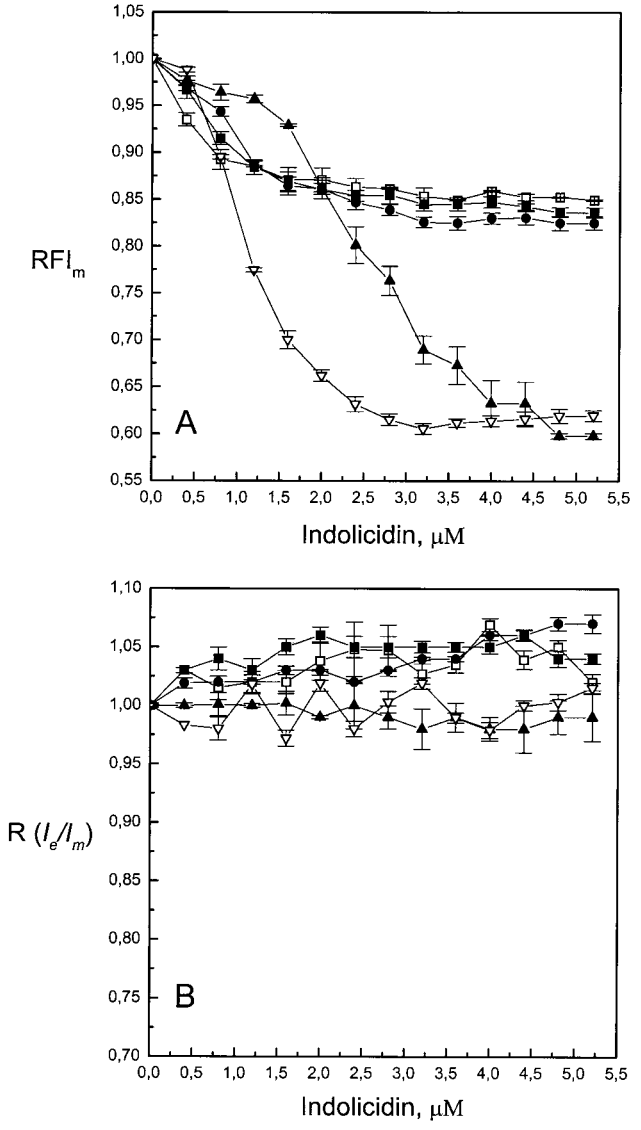

FIGURE 4 Effects of indolicidin on lipid dynamics in LUVs assessed by pyrene-labeled phospholipid analogs, depicted as changes in pyrene monomer emission intensity $I_m \approx 398$ nm (*A*) and excimer to monomer ratio $R(I_e/I_m)$ (*B*). PPDPC was used in SOPC and SOPC/cholesterol LUVs and PPDPG in LUVs containing POPG. Liposomes were composed of SOPC with $X_{PG} = 0$ (□), 0.1 (■), 0.2 (●), and 0.4 (▲) and with $X_{chol} = 0.1$ (▼). Otherwise, conditions were as described in the legend for Fig. 2.

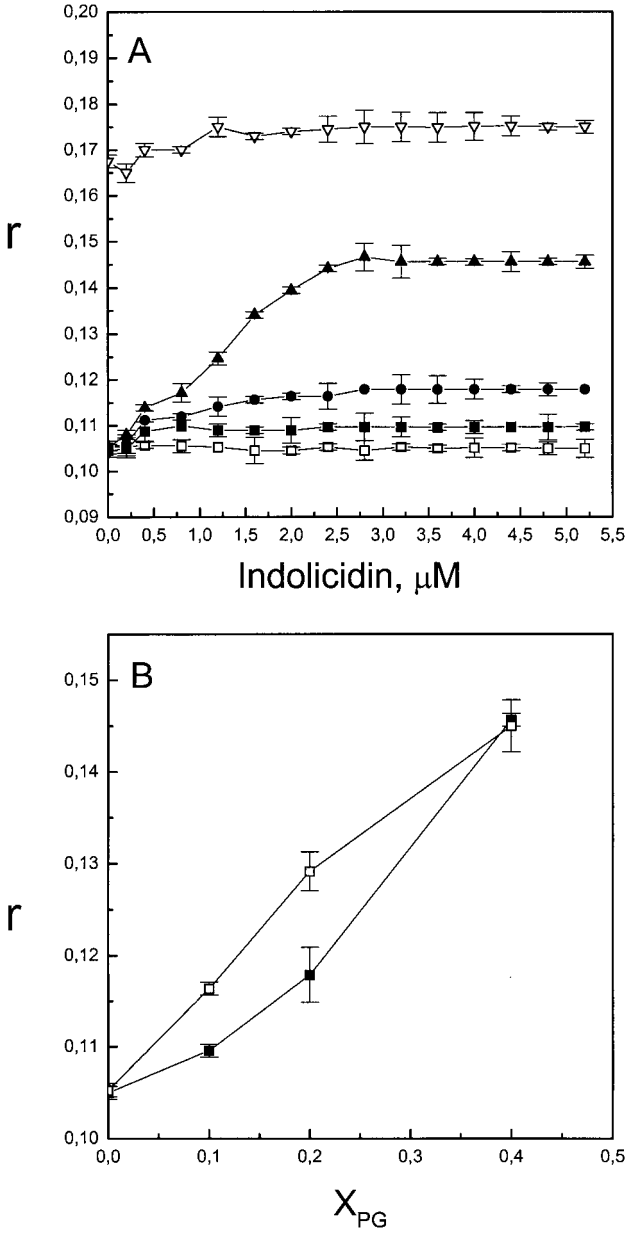

FIGURE 5 Effects of indolicidin on the steady-state emission anisotropy *r* of DPH ($X = 0.002$) (*A*) in SOPC liposomes with $X_{PG} = 0$ (■), 0.1 (□), 0.2 (●), and 0.4 (▲) and with $X_{chol} = 0.1$ (▲). The changes in *r* as a function of X_{PG} upon addition of 3.6 μM indolicidin (■) are shown in *B*. For comparison, the data for magainin 2 (□) are also shown. Otherwise, conditions were as described in the legend for Fig. 2.

composed of SOPC and cholesterol ($X_{chol} = 0.1$) were unaffected by this quantity of magainin 2 (data not shown). However, in the presence of POPG ($X_{PG} = 0.1$) already ~0.01 fmol (a single ~20-fl injection) of magainin 2 applied onto the surface of giant vesicles significantly affected the topology of the giant liposome membrane (Fig. 6 *B*). More specifically, in ~1 min, small particles ($\phi \approx 0.9$ μm) emerged inside the giant vesicle. Subsequent injections of magainin 2 up to ~0.1 fmol (in ~200 fl) caused no further visible changes. After the addition of a total of ~0.2 fmol of the peptide, the membrane began to undulate and a dense particle ($\phi \approx 4$ μm) became visible inside the giant liposome (Fig. 6 *C*). In ~5 min, several small particles ($\phi \approx 0.9$ μm) emerged on the inner surface of the giant liposome membrane (Fig. 6 *D*). Subsequently, most of these small particles moved into the internal cavity of the giant vesicle. These endocytotic vesicles appeared to move freely inside the giant liposome, with no further changes during the following 30 min of observation. Further injection of ma-

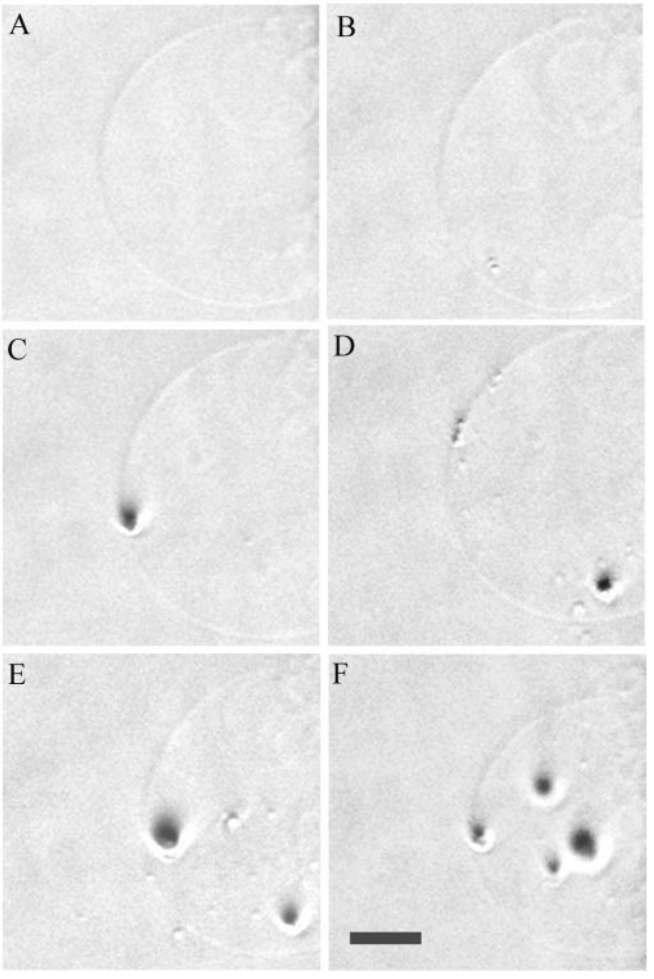

FIGURE 6 HMC images of transformation induced by magainin of a SOPC/POPG (X_{PG} = 0.1) giant liposome. Shown is a giant vesicle before the addition of magainin (*A*), 1 min after the addition of ~0.01 fmol of magainin (*B*), after the addition of a total of ~0.2 fmol of magainin (*C*), after 5 min (*D*), 10 min after the addition of a total of ~0.3 fmol of magainin (*E*), and immediately after the addition of a total of ~0.7 fmol of magainin (*F*). The length of the scale bar in *F* corresponds to 20 μm.

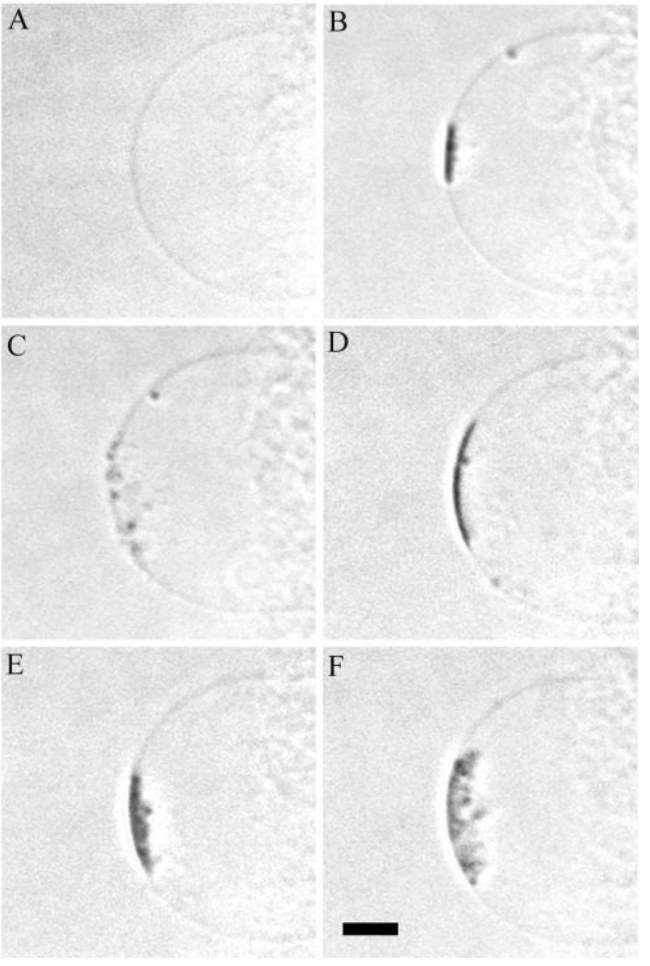

FIGURE 7 HMC images of transformation induced by indolicidin of a SOPC/POPG (X_{PG} = 0.1) giant liposome. Shown is a giant vesicle before the addition of the peptide (*A*) and immediately (*B*) and 1 min (*C*) after the addition of ~0.5 fmol of indolicidin. Subsequent images were taken immediately (*D*), 1 min (*E*), and 2 min (*F*) after the addition of a total of ~0.6 fmol of indolicidin. The length of the scale bar in *F* corresponds to 20 μm.

gainin 2 delivering a total of 0.3 fmol of the peptide caused an endocytosis-like process with the emergence of a dense particle with a diameter of ~8 μm (Fig. 6 *E*). The number of the ~0.9-μm particles inside the giant liposomes continued to increase after ~10 min. Occasionally, these particles emerged also on the outer surface of the giant vesicle and were released into the external buffer (Fig. 6 *E*). Subsequent addition of magainin 2 (~0.7 fmol in total) destabilized the membrane and induced further vesiculation (Fig. 6 *F*). These endocytotic vesicles remained separated from each other inside the giant liposome, and the size of the giant vesicle decreased visibly (Fig. 6 *F*). Eventually, upon further addition of magainin 2 (up to ~1.5 fmol) the giant liposome membrane collapsed. The above morphological changes were highly reproducible.

Subsequently, we studied the effects of indolicidin on giant liposomes composed of SOPC as well as of its mixtures with POPG (X_{PG} = 0.1). For SOPC giant liposomes the only change evident was a minor shrinkage after the application of ~2 fmol (~200 injections) of indolicidin onto their surface (data not shown). However, when the vesicle contained POPG (X = 0.1), indolicidin (~0.5 fmol) induced an endocytosis-like process (Fig. 7) and small particles (ϕ ~ 0.9 μm) appeared inside the giant liposome. After the addition of ~0.5 fmol of indolicidin (50 injections) the area of the giant liposome surface exposed to indolicidin became dark, revealing a pronounced change in the refractive index and indicating the formation of a tightly packed three-dimensional structure, remaining only partly in the focal plane (Fig. 7 *B*). Small particles ($\phi \approx$ 0.9 μm) emerged inside the giant liposome within ~1 min after the

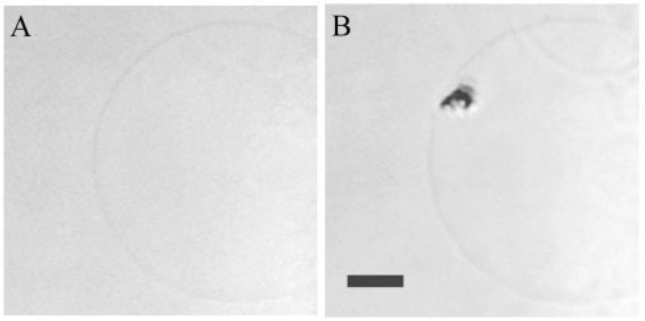

FIGURE 8 HMC microscopy images of giant liposomes in the presence of cholesterol ($X_{chol} = 0.1$) following application of indolicidin onto their surface. The images were recorded before (*A*) and 5 s after (*B*) the addition of ~0.2 fmol of indolicidin, respectively. The length of the scale bar in *D* corresponds to 20 μm.

formation of the above aggregate (Fig. 7 *C*). The aggregate on the surface of the membrane remained after the subsequent addition of another 0.1 fmol of indolicidin, with more of the small-diameter particles emerging inside the giant vesicle (Fig. 7, *D–F*). This endocytosis-like process was repeated with subsequent addition of indolicidin, with progressive accumulation of a number of small particles inside the giant liposome and with the size of the giant liposome decreasing slightly.

Subsequently, we studied the impact of indolicidin on giant liposomes composed of SOPC and cholesterol ($X_{chol} = 0.1$). Indolicidin caused vesiculation of giant liposome also in the presence of cholesterol. The endocytotic vesicles formed were profoundly aggregated on the surface of the giant vesicle (Fig. 8 *B*). Specifically, within ~5 s after the addition of ~0.2 fmol of indolicidin (~400 fl, 20 injections, Fig. 8 *B*), a cluster of small particles emerged on the surface of the giant liposome. Subsequently, the aggregate transferred into the giant liposome, while also a few endocytotic particles ($\phi \approx 0.9$ μm) were visible. Further addition of indolicidin increased the number of these particles and caused shrinkage of the giant liposome. However, the membrane remained macroscopically intact even when exposed to ~2 fmol of indolicidin (200 injections, data not shown).

DISCUSSION

Membrane activities of magainin 2 and indolicidin

Monolayer experiments revealed magainin 2 and indolicidin to be highly membrane active (Fig. 1), producing significant increment in surface pressure following their injection underneath lipid films residing on an air/water interface. Depending on film composition, critical packing densities corresponding to surface pressures π_c were found above which these peptides could no longer interact with the monolayers in a manner producing increase in π (Verger and Pattus, 1976). Although both peptides intercalated into zwitterionic phosphatidylcholine monolayers, they interact preferentially with acidic phospholipids, in keeping with their net cationic charge (Matsuzaki et al., 1991, 1993, 1995a, 1998; Ladokhin et al., 1997). Yet, the impact of PG on their penetration was significantly different, with a crossover point at a surface pressure of ~38 mN/m being evident for indolicidin, the slopes for $\Delta\pi$ versus π_0 becoming steeper in the presence of PG (Fig. 1). In contrast, the slopes for $\Delta\pi$ versus π_0 for the penetration of magainin 2 remained unaltered by the presence of PG (Fig. 1 *A*). Our data suggest that magainin 2 attaches more superficially with the monolayer, its penetration depth being increased by PG and progressively reduced with increasing surface pressure, with the angle of its long axis with respect to the layer plane remaining relatively unaltered at different pressures. The above mode of interaction of magainin 2 with lipid monolayers would be compatible 1) with its predominately α-helical conformation, the degree of α-helicity being increased by PG (Wieprecht et al., 1997), and 2) the shallow penetration of this peptide into lipid bilayers with its long axis parallel to the layer plane (Bechinger et al., 1993; Matsuzaki et al., 1994). At $\pi > \pi_c$ magainin 2 may still associate electrostatically with the PG in the monolayer, although without penetrating into the film and thus causing no increment in π. Finally, our data also suggest that unlike in bilayers, magainin 2 would not adopt the vertical orientation (i.e., the long axis of its α-helix perpendicular to the layer plane) in lipid monolayers.

For all monolayer compositions tested the values of π_c for indolicidin exceeded those measured for magainin 2 (Fig. 1 *C*), revealing effective insertion and intercalation of this peptide between the acyl chains. The crossover point at ~38 mN/m for indolicidin is of interest. Below the latter surface pressure the increment in surface pressure $\Delta\pi$ caused by indolicidin was augmented in the presence of PG whereas the opposite was observed at higher initial lipid packing densities. Intriguingly, the crossover point remains virtually unaltered irrespective of lipid composition (i.e., presence of PG), thus suggesting that it could be solely determined by surface pressure, irrespective of electrostatic interactions. A possible mechanism is that at $\pi_0 > 38$ mN/m indolicidin changes its orientation in the monolayer in a pressure-dependent manner, perhaps from a parallel to perpendicular orientation of its long axis with respect to the layer plane (Fig. 9, *B* and *C*), thus reducing the area/peptide and decreasing $\Delta\pi$. Furthermore, it is also possible that some PG molecules that are electrostatically bound to indolicidin become oriented differently from the phospholipids in the monolayer. In other words, indolicidin with its associated PG would form a supramolecular complex, the orientation of which would be pressure dependent. This is schematically illustrated in Fig. 9. Importantly, the proposed reorientation of peptide-attached phospholipids would be compatible with the recently suggested model in which part of the surface of the pore traversing the bilayer

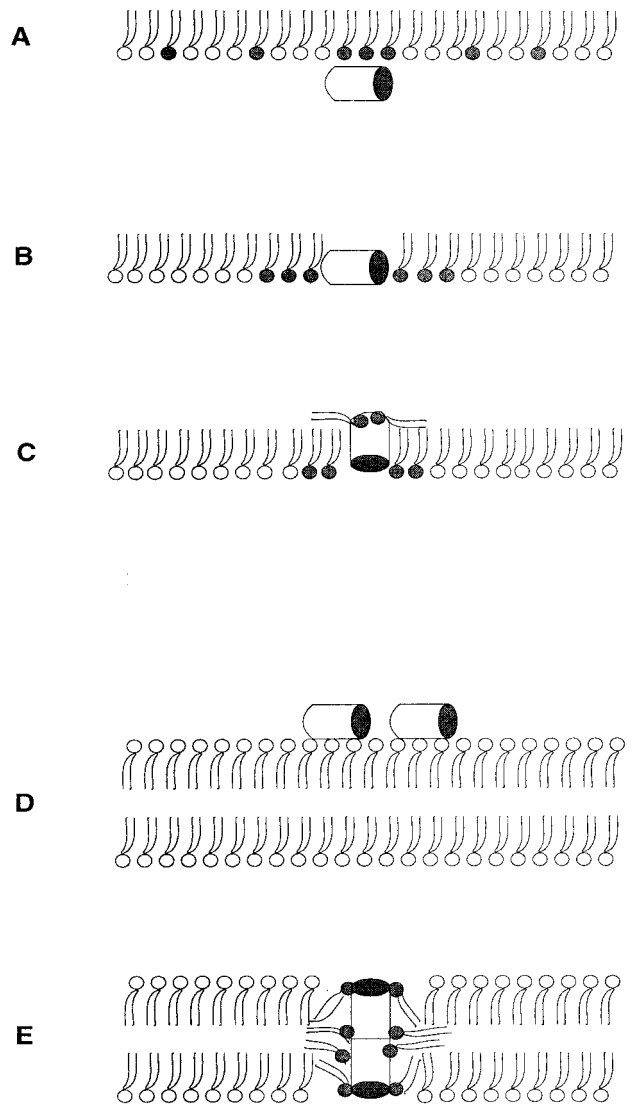

FIGURE 9 Model depicting the interactions of indolicidin with lipid monolayers and bilayers. (*A*—*C*) Association of indolicidin with lipid monolayers; (*D* and *E*) Interaction of indolicidin with lipid bilayers in. The filled spheres represent the negatively charged lipid headgroups, and the open spheres represent the zwitterionic lipid headgroups. The molecules of indolicidin are illustrated as small cylinders.

would be constituted by lipid headgroups (Ludtke et al., 1996).

Impact of magainin 2 and indolicidin on bilayer lipid dynamics

Although distinct differences were revealed by fluorescence spectroscopy in the effects of magainin 2 and indolicidin on lipid dynamics, also several similarities were evident. Accordingly, increment in DPH anisotropy r showed that both peptides cause an increase in acyl chain order in the presence of the acidic phospholipid, the magnitude of this effect increasing with X_{PG} (Figs. 3 *B* and 5 *B*). Likewise, efficient quenching of pyrene fluorescence by both peptides was evident in the presence of cholesterol (Figs. 2 *A* and 4 *A*). This may relate to the suggested interaction between the OH group of cholesterol and residue E19 of magainin (Tytler et al., 1995), with a transmembrane orientation of the peptide in the membrane. At $X_{chol} = 0.1$, augmented values of r were due to indolicidin whereas magainin was without effect. This suggests that also in the presence of cholesterol, indolicidin may adopt a transbilayer orientation, its long axis perpendicular to the plane of the bilayer.

The mechanisms of quenching of the pyrene-labeled phospholipid analogs by the two antimicrobial peptides are of interest. π-Cation interactions could be involved (Dougherty, 1996), the latter being represented by the basic residues of the peptides. Indolicidin has a high content of Trp (39%), which could promote its partitioning into the lipid bilayer (Wimley and White, 1996). Accordingly, also π-π interactions between pyrene and Trp are possible. It has been demonstrated that Trp can quench fluorescence emission of various pyrene derivatives in micellar solutions (Encinas and Lissi, 1986; Altamirano et al., 1998). An additional possibility is chain reversal (Holopainen et al., 1999) causing accommodation of the pyrene moiety into a more polar environment upon the binding of the peptide to the lipid bilayer, thus increasing the polarity of the microenvironment of the fluorophore and causing decrement in quantum yield.

In addition to the above similarities, also pronounced differences between the two peptides were evident when the effects of the acidic phospholipid on lipid dynamics were investigated with the pyrene-labeled lipid analogs. Magainin 2 caused significant quenching of the pyrene emission for LUVs composed of zwitterionic phospholipids (Fig. 2 *A*). However, in the presence of PG, the monomer intensity of pyrene increased, the magnitude of this effect being progressively augmented with X_{PG} (Fig. 2 *A*). Circular dichroism, Raman, Fourier transform infrared, and solid-state nuclear magnetic resonance studies show that magainin adopts an α-helical conformation upon binding to lipid bilayers (Matsuzaki et al., 1989, 1991; Williams et al., 1990; Jackson et al., 1992; Bechinger et al., 1993; Wieprecht at al., 1997; Hirsh et al., 1996). These different effects of magainin 2 on the two membranes may be due to 1) quenching of pyrene fluorescence by direct contacts with the positively charged groups of the peptide, e.g., the ϵ-amino group of lysine, or 2) the microenvironment of the fluorophore being changed by the α-helical peptide residing inserted into the bilayer, parallel to the layer plane, as outlined above. In the presence of PG, however, the positive charges of the peptide should be neutralized upon electrostatic complex formation with the acidic phospholipid, thus reducing the quenching of pyrene fluorescence due to π-cation interactions.

Interestingly, in the presence of the acidic phospholipid, the magainin/lipid molar ratios at which the initial increment in I_m leveled off were 1:21, 1:16, and 1:12.5, corresponding to $X_{PG} = 0.1$, 0.2, and 0.4 (Fig. 2 *A*), yielding magainin/PG stoichiometries of 1:2, 1:3, and 1:5, respectively. In parallel, the initial increment in r for DPH leveled off at magainin/lipid molar ratios of ~1:30, 1:12, and 1:5 (at $X_{PG} = 0.1$, 0.2, and 0.4, respectively), corresponding to approximate magainin/PG stoichiometries of 1:3, 1:2.5, and 1:2 (Fig. 3). At these peptide/lipid molar ratios, magainin has been reported to insert into acidic-phospholipid-containing membranes (Ludtke et al., 1994). Moreover, it has been shown that the orientation of the α-helix of magainin in a bilayer depends on the peptide:lipid molar ratios, and at the above stoichiometries the helices should insert perpendicular to the membrane surface, forming pores in PG-containing membranes (Ludtke et al., 1996). The pores have been suggested to be composed of not only the polar face of the amphiphilic helices but also of the polar headgroup of the lipids, with the inner and outer monolayers being continuous via these pore-lining lipids. This structure in the membrane may reduce the polarity of the microenvironment for the pyrene moiety of the probes and thus increase its quantum yield. Interestingly, the values for I_e/I_m were progressively decreased by magainin 2 at $X_{PG} > 0.1$ (Fig. 3 *A*), in keeping with the enhanced acyl chain order diminishing the rate of lipid lateral diffusion. Yet, as r was increased by magainin 2 already at $X_{PG} = 0.1$, with no changes in I_e/I_m, we may conclude that both enrichment of the PPDPG probe into microdomains as well as reduction in its lateral diffusion are taking place.

Similarly to magainin 2, the membrane association of indolicidin with anionic and zwitterionic vesicles was quite different (Figs. 1 *B*, 4, and 5), in keeping with previous equilibrium dialysis studies (Ladokhin et al., 1997). Whereas quenching of pyrene fluorescence revealed partitioning of indolicidin into a SOPC bilayer it had little effect on membrane acyl chain order (Fig. 5). Instead, the interaction of indolicidin with anionic membranes causes augmented lipid acyl chain order, evident as an increase in DPH fluorescence anisotropy and with sigmoidal dependence on X_{PG} (Fig. 5). In contrast to magainin 2, indolicidin caused significant and parallel decrease in both pyrene monomer and excimer emission intensities, independently from lipid composition, and with minor changes in I_e/I_m (Fig. 4). Accordingly, enrichment of the acidic PG into microdomains is induced by indolicidin. Interestingly, below indolicidin/lipid molar ratio of 1:20, pyrene I_m decreased in the sequence $X_{PG} = 0.4 < 0.2 < 0.1 < 0$ (Fig. 4 *A*), whereas at indolicidin/lipid molar ratio of 1:10 the dependence of the decrement in I_m on X_{PG} was reversed. A possible mechanism for this change could be the following. At low peptide/lipid molar ratio indolicidin appears to become accommodated into the bilayer interface (Ladokhin et al., 1997), with chain reversal (Holopainen et al., 1999) of the pyrene-labeled chain bringing this moiety closer to the bilayer surface and thus allowing its contact with the basic residues of indolicidin. The latter would thus cause collisional quenching of the pyrene moiety by π-cation interactions. However, with increasing X_{PG} we can expect electrostatic binding of PG headgroups to the basic residues of indolicidin, thus preventing direct contacts between pyrene and the cationic residues of indolicidin. As the membrane binding of indolicidin is augmented in a cooperative manner with increasing peptide concentration, the reversal of the efficiency in quenching could involve clustering of the lipid-peptide complexes in the bilayer. Quenching of pyrene by indolicidin would therefore be less in acidic-phospholipid-containing membranes. When the concentration of indolicidin increases above the peptide/lipid ratio of 1:10, the peptide would incorporate in a highly cooperative manner within the acyl chain region of the membrane (Ha et al., 2000) (Fig. 9 *E*), whereas in neutral membranes it locates in the interface (Fig. 9 *D*). The amount of inserted indolicidin would depend on X_{PG} in the bilayer, causing the quenching by Trp residues of indolicidin to dominate, in keeping with the pronounced decrement in I_m at $X_{PG} = 0.4$ (Fig. 4 *A*).

Effects of magainin 2 and indolicidin on giant liposomes

Cytoplasmic membrane permeabilization is considered to be responsible for the antimicrobial action of peptides such as magainin and indolicidin (Matsuzaki, 1998, 1999; Sitaram and Nagaraj, 1999), and several models for its mechanism have been proposed (for a review, see Bechinger, 1999). Pore or channel formation has been suggested to cause dissipation of transmembrane potential and lipid asymmetry (Falla et al., 1996; Matsuzaki, 1998, 1999; Sitaram and Nagaraj, 1999). Magainin 2 and indolicidin should insert into the lipid bilayers as defined structures, in a conformation with all hydrophobic amino acids constituting one surface that then contacts the hydrophobic core of the membrane. Membrane insertion of these peptides thus forces the phospholipid acyl chains apart. The antimicrobial actions of these peptides may also include local phase transitions, such as the separation of lipid-peptide micelles from the bilayers, or local changes of the membrane curvature due to the intercalating peptides, which could cause a local collapse of the bilayer structure. On a molecular level these processes could be underlying the vesiculation of giant vesicles induced by magainin 2 and indolicidin reported here. The lytic activity of magainin is highly sensitive to the lipid composition of the target membrane, and this peptide preferentially binds to and permeabilizes anionic-lipid-containing membranes (Matsuzaki et al., 1991, 1993, 1995a, 1998). Accordingly, magainin at concentrations lethal to microorganisms does not lyse mammalian cells, which do not contain negatively charged phospholipids in the outer monolayer of their plasma membrane (Ma-

tsuzaki, 1999). The exposure of *E. coli* to magainin causes blebs on the bacterial surface (Matsuzaki et al., 1997). In the present study, vesiculation of giant liposomes induced by magainin 2 and indolicidin was observed, representing more macroscopic changes of their binding to lipid bilayers. Importantly, the presence of the acidic PG was required for vesiculation by both peptides. Vesiculation of giant liposomes required repeated applications of magainin 2 and thus imply a concentration-dependent mechanism of action. It has been demonstrated that the pores formed in the presence of magainin are transient, with a finite lifetime (Matsuzaki et al., 1995b). Upon disintegration of nearby pores, a supramolecular complex of peptides and lipids may form, thus causing transient disruption of the bilayer (Fig. 6). Simultaneously, some of the peptide molecules should translocate into the inner leaflet of the membrane (Matsuzaki et al., 1995a, 1996), allowing the membrane to reorganize and heal. Formation of endocytotic vesicles due to magainin 2 is more pronounced than exocytosis (Fig. 6), which may relate to the asymmetric application of the peptide onto the outer surface of the bilayer. Accordingly, the vesiculation of the giant liposome could relieve the bilayer from unfavorable strain due to the asymmetrical peptide binding and subsequent membrane expansion. Vesiculation can be expected to decrease the peptide concentration in the remaining giant liposome membrane and thus attenuate pore formation. Subsequently, continued addition of magainin 2 to the membrane is needed to cause further vesiculation of the giant liposome (Fig. 6).

Indolicidin contains only 13 amino acids and as such is too short to span the bilayer. Yet, the peptide could span the bilayer as an aggregate or a head-to-tail dimer with associated acidic phospholipids (Fig. 9 *E*), inducing membrane instability. It has been shown that indolicidin is capable of killing Gram-negative bacteria by crossing the outer membrane as well as causing disruption of the cytoplasmic membrane, with the formation of channels (Falla et al., 1996). Compared with the effects of magainin 2 the smaller size of the endocytotic vesicles induced by indolicidin (Fig. 7) may reflect different modes of interaction of these peptides with lipids. Some of the indolicidin molecules may translocate into the inner leaflet of the membrane. In addition to its broad spectrum of antifungal and antibacterial activities, indolicidin is also toxic to mammalian cells (Schluesener et al., 1993; Ahmad et al., 1995). Interestingly, the effects of indolicidin on SOPC and SOPC-cholesterol giant liposomes differ. The underlying cause is uncertain at this stage and could relate to the impact of cholesterol on the bilayer structure as well as on the orientation of indolicidin in the membrane. Further studies are thus needed to elucidate the effect of cholesterol on the membrane binding of indolicidin.

Our results show that the effects of magainin 2 on the biomembrane models used were significantly enhanced in the presence of the negatively charged phospholipid. In addition to the negative membrane charge, also the peptide/lipid stoichiometry has been shown to be an important determinant for the organization of magainin in bilayers (Ludtke et al., 1994). At low peptide/lipid ratio, the α-helical peptide lies essentially parallel to the membrane surface and shallowly penetrating into the hydrophobic core of the membrane (Bechinger et al., 1993; Matsuzaki et al., 1994). This location pushes the lipid headgroups aside, forcing a gap to form in the hydrophobic region, while the membrane becomes thinner to fill the gap (Ludtke et al., 1995). The transient nature of the pores formed by magainin has been emphasized previously (Matsuzaki et al., 1995b). It is possible that the local and transient disruption of the membrane requires asymmetric binding of the peptide to the target cell membrane. Accordingly, immediately following the binding of magainin to the outer leaflet of the target cell plasma membrane bilayer the lateral pressure of this outer monolayer increases compared with the inner leaflet. Moreover, the superficial location of the α-helices parallel to the layer plane imposes curvature strain in the outer monolayer, causing positive spontaneous curvature. When the magnitude of lateral pressure difference between the two leaflets and energy associated with the positive spontaneous curvature exceed the energy needed for membrane deformation, the bilayer is destabilized and reorientation of the peptide to vertical orientation with respect to layer plane takes place, with opening of pores. These pores may subsequently aggregate into supramolecular structures inside the target, as observed in giant liposomes (Fig. 6). The pores and the destabilized state would thus be transient, allowing healing of the bilayer. To this end, magainin 2 contains a cluster of positive charges approximately in the middle of its sequence. It is possible that also when this peptide is forming the transient pore in bilayers and is oriented perpendicular to the membrane plane, these cationic residues would be electrostatically bound to PG, similarly to the organization proposed here for indolicidin (Fig. 9). A major difference in lipid composition of membranes between prokaryotic and eukaryotic cells is that the latter are abundant in cholesterol (Op den Kamp, 1979). The above mechanism would also be compatible with the presence of cholesterol preventing the membrane-perturbing action of magainin 2. More specifically, cholesterol has been shown to transfer (flip-flop) very fast between the two leaflets of human plasma membrane (Lange et al., 1981). Accordingly, this rapid translocation of cholesterol could abolish the generation of difference in the lateral pressure of the inner and outer leaflet of the target membrane following the binding of magainin 2 into the latter monolayer. Therefore, significantly higher amounts of magainin 2 would be needed to achieve toxic effects by this peptide in eukaryotic cells compared with bacterial targets (Zasloff, 1987). The equilibrium lateral pressure in the outer leaflet of the eukaryotic plasma membranes has been estimated to be $\sim$32 mN/m (Demel et al., 1975). The observed highly efficient penetration of indolicidin into monolayers

at pressures exceeding 34 mN/m may explain in part the lytic action of this peptide in eukaryotic cells. Moreover, the outer leaflet of mammalian plasma membranes is exclusively composed of zwitterionic phospholipids, whereas bacterial membranes contain large amounts of negatively charged PG (Op den Kamp, 1979). Accordingly, because of the lack of negative charges and high pressure only weak interaction of magainin 2 with eukaryotic plasma membrane would be expected whereas the much more efficiently intercalating indolicidin would be able to perturb the organization of eukaryotic bilayers. The lipid specificity could thus contribute to the different toxicities of these two peptides.

CONCLUSIONS

As the detailed mechanisms of action of antimicrobial peptides remain to be elucidated, it was of interest to compare the effects on model biomembranes of two structurally unrelated peptides, indolicidin and magainin 2. Although their conformations are different and the length of the former is approximately one half of that of the latter, they also share features such as net positive charge and amphiphilicity, causing them to associate with phospholipid membranes. This interaction is further enhanced by acidic phospholipids, which are probably important to their antimicrobial activity. Acidic phospholipids were required for the vesiculation of giant liposomes by these peptides, and they both cause segregation of acidic phospholipids, complexing them into supramolecular clusters. Likewise, both peptides increase acyl chain order. All these effects are in keeping with cooperative membrane association being necessary for their antimicrobial action, presumably involving transient transmembrane orientation of the peptides. It may further be that their antimicrobial action requires the initially asymmetric exposure of the target membranes to these peptides and relates to the relaxation of the system back to thermodynamic equilibrium.

We thank Kaija Niva for skillful technical assistance. We are grateful to Dr. Nisse Kalkkinen (Protein Chemistry Laboratory, Institute of Biotechnology, University of Helsinki) for mass spectroscopy analyses of the peptides.

This study was supported by Technology Development Fund (TEKES), and the Finnish Academy.

REFERENCES

Ahmad, I. W., R. Perkins, D. M. Lupan, M. E. Selsted, and A. S. Janoff. 1995. Liposomal entrapment of the neutrophil-derived peptide indolicidin endows it with in vivo antifungal activity. *Biochim. Biophys. Acta.* 1237:109–114.

Aley, S. B., M. Zimmerman, M. Hetsko, M. E. Selsted, and F. D. Gillin. 1994. Killing of *Giardia lamblia* by cryptdins and cationic neutrophil peptides. *Infect. Immun.* 62:5397–5403.

Altamirano, M. S., C. D. Borsarelli, J. J. Cosa, and C. M. Previtali. 1998. Influence of polarity and viscosity of the micellar interface on the fluorescence quenching of pyrenic compounds by indole derivatives in AOT reverse micelles solution. *J. Colloid Interface Sci.* 205:390–396.

Angelova, M. I., and D. S. Dimitrov. 1986. Liposome electroformation. *Faraday Discuss. Chem. Soc.* 81:303–311.

Angelova, M. I., N. Hristova, and I. Tsoneva. 1999. DNA-induced endocytosis upon local microinjection to giant unilamellar cationic vesicles. *Eur. Biophys. J.* 28:142–150.

Angelova, M. I., and I. Tsoneva. 1999. Interactions of DNA with giant liposomes. *Chem. Phys. Lipids.* 101:123–137.

Baker, M. A., W. L. Maloy, M. Zasloff, and L. S. Jacob. 1993. Anticancer efficacy of magainin2 and analogue peptides. *Cancer Res.* 53: 3052–3057.

Bechinger, B. 1997. Structure and functions of channel-forming peptides: magainin, cecropins, mellitin and alamethicin. *J. Membr. Biol.* 156: 197–211.

Bechinger, B. 1999. The structure, dynamics, and orientation of antimicrobial peptides in membranes by multidimensional solid-state NMR spectroscopy. *Biochim. Biophys. Acta.* 1462:157–183.

Bechinger, B., M. Zasloff, and S. J. Opella. 1993. Structure and orientation of the antibiotic peptide magainin in membranes by solid-state nuclear magnetic resonance spectroscopy. *Protein Sci.* 2:2077–2084.

Brockman, H. 1999. Lipid monolayers: why use half of a membrane to characterize protein-membrane interactions? *Curr. Opin. Struct. Biol.* 9:438–443.

Cruciani, R. A., J. L. Barker, M. Zasloff, H.-C. Chen, and O. Colamonici. 1991. Antibiotic magainins exert cytolytic activity against transformed cell lines through channel formation. *Proc. Natl. Acad. Sci. U.S.A.* 88:3792–3796.

Demel, R. A., W. S. M. Geurts van Kessel, R. F. A. Zwaal, B. Roelofsen, and L. L. M. Van Deenen. 1975. Relation between various phospholipase actions on human red cell membranes and the interfacial phospholipid pressure in monolayers. *Biochim. Biophys. Acta.* 406:97–107.

Dougherty, D. A. 1996. Cation-π interactions in chemistry and biology: a new view of benzene, Phe, Tyr, and Trp. *Science.* 271:163–168.

Duportail, G., and P. Lianos. 1996. Fluorescence probing of vesicles using pyrene and pyrene derivatives. *In* Vesicles. M. Rosoff, editor. Marcel Decker, New York. 295–372.

Encinas, M. V., and E. A. Lissi. 1986. Quenching of pyrene fluorescence by tryptophan in micellar solutions. *Photochem. Photobiol.* 44:579–585.

Falla, T. J., D. N. Karunaratne, and R. E. W. Hancock. 1996. Mode of action of the antimicrobial peptides indolicidin. *J. Biol. Chem.* 271: 19298–19303.

Ha, T. H., C. H. Kim, J. S. Park, and K. Kim. 2000. Interaction of indolicidin with model lipid bilayer: quartz crystal microbalance and atomic force microscopy study. *Langmuir.* 16:871–875.

Hirsh, D. J., J. Hammer, W. L. Maloy, J. Blazyk, and J. Schaefer. 1996. Secondary structure and location of a magainin analogue in synthetic phospholipid bilayers. *Biochemistry.* 35:12733–12741.

Holopainen, J. M., M. I. Angelova, and P. K. J. Kinnunen. 2000. Vectorial budding of vesicles by asymmetrical enzymatic formation of ceramide in giant liposomes. *Biophys. J.* 78:830–838.

Holopainen, J. M., J. Y. A. Lehtonen, and P. K. J. Kinnunen. 1999. Evidence for the extended phospholipid conformation in membrane fusion and hemifusion. *Biophys. J.* 76:2111–2120.

Jackson, M., H. H. Mantsch, and J. Spencer. 1992. Conformation of magainin-2 and related peptides in aqueous solution and membrane environments probed by Fourier transform infrared spectroscopy. *Biochemistry.* 31:7289–7293.

Kinnunen, P. K. J., A. Koiv, and P. Mustonen. 1993. Pyrene-labeled lipids as fluorescent probes in studies on biomembranes and membrane models. *In* Fluorescence Spectroscopy. O. S. Wolfbeis, editor. Springer Verlag, New York. 159–171

Ladokhin, A. S., M. E. Selsted, and S. H. White. 1997. Bilayer interactions of indolicidin, a small antimicrobial peptide rich in tryptophan, proline, and basic amino acids. *Biophys. J.* 72:794–805.

Ladokhin, A. S., M. E. Selsted, and S. H. White. 1999. CD spectra of indolicidin antimicrobial peptides suggest turns, not polyproline helix. *Biochemistry.* 38:12313–12319.

Lange, Y., J. Dolde, and T. L. Steck. 1981. The rate of transmembrane movement of cholesterol in the human erythrocyte. *J. Biol. Chem.* 256:5321–5323.

Ludtke, S. J., K. He, W. T. Heller, T. A. Harroun, L. Yang, and H. W. Huang. 1996. Membrane pores induced by magainin. *Biochemistry.* 35:13723–13728.

Ludtke, S. J., K. He, and H. W. Huang. 1995. Membrane thinning caused by magainin 2. *Biochemistry.* 34:16764–16769.

Ludtke, S. J., K. He, Y. Wu, and H. W. Huang. 1994. Cooperative membrane insertion of magainin correlated with its cytolytic activity. *Biochim. Biophys. Acta.* 1190:181–184.

Luisi, P. L., and P. Walde. 2000. Giant Vesicles. John Wiley and Sons, Chichester, UK.

Matsuzaki, K. 1998. Magainins as paradigm for the mode of action of pore forming polypeptides. *Biochim. Biophys. Acta.*1376:391–400.

Matsuzaki, K. 1999. Why and how are peptide-lipid interactions utilized for self-defense? Magainins and tachyplesins as archetypes. *Biochim. Biophys. Acta.* 1462:1–10.

Matsuzaki, K., M. Harada, S. Funakoshi, N. Fujii, and M. Miyajima. 1991. Physicochemical determinants for the interactions of magainins 1 and 2 with acidic lipid bilayers. *Biochim. Biophys. Acta.* 1063:162–170.

Matsuzaki, K., M. Harada, T. Handa, S. Funakoshi, N. Fujii, H. Yajima, and K. Miyajima. 1989. Magainin 1-induced leakage of entrapped calcein out of negatively-charged lipid vesicles. *Biochim. Biophys. Acta.* 981:130–134.

Matsuzaki, K., O. Murase, N. Fujii, and M. Miyajima. 1995b. Translocation of a channel-forming antimicrobial peptide, magainin 2, across lipid bilayers by forming a pore. *Biochemistry.* 34:6521–6526.

Matsuzaki, K., O. Murase, N. Fujii, and M. Miyajima. 1996. An antimicrobial peptide, magainin 2, induced rapid flip-flop of phospholipids coupled with pore formation and peptide translocation. *Biochemistry.* 35:11361–11368.

Matsuzaki, K., O. Murase, and M. Miyajima. 1995c. Kinetics of pore formation by an antimicrobial peptide, magainin 2, in phospholipid bilayers. *Biochemistry.* 34:12553–12559.

Matsuzaki, K., O. Murase, H. Tokuda, S. Funakoshi, N. Fujii, and K. Miyajima. 1994. Orientational and aggregational states of magainin 2 in phospholipid bilayers. *Biochemistry.* 33:3342–3349.

Matsuzaki, K., M. Nakayama, M. Fukui, A. Otaka, S. Funakoshi, N. Fujii, K. Bessho, and K. Miyajima. 1993. Role of disulfide linkages in tachyplesin-lipid interactions. *Biochemistry.* 32:11704–11710.

Matsuzaki, K., K. Sugishita, N. Fujii, and K. Miyajima. 1995a. Molecular basis for membrane selectivity of an antimicrobial peptide, magainin 2. *Biochemistry.* 34:3423–3429.

Matsuzaki, K., K. Sugishita, M. Harada, N. Fujii, and M. Miyajima. 1997. Interactions of an antimicrobial peptide, magainin 2, with outer and inner membranes of Gram-negative bacteria. *Biochim. Biophys. Acta.* 1327:119–130.

Matsuzaki, K., K. Sugishita, N. Ishibe, M. Ueha, S. Nakata, K. Miyajima, and R. M. Epand. 1998. Relationship of membrane curvature to the formation of pores by magainin 2. *Biochemistry.* 37:11856–11863.

Menger, F. M. 1998. Giant vesicles: imitating the cytological processes of cell membranes. *Acc. Chem. Res.* 31:789–797.

Menger, F. M., and J. S. Keiper. 1998. Giant vesicles: micromanipulation of membrane bilayers. *Advanced Materials*. 10:888–890.

Menger, F. M., and S. J. Lee. 1995. Induced morphological changes in synthetic giant vesicles: growth, fusion, undulation, excretion, wounding, and healing. *Langmuir.* 11:3685–3689.

Op den Kamp, J. A. 1979. Lipid asymmetry in membranes. *Annu. Rev. Biochem.* 48:47–71.

Oren, Z., and Y. Shai. 1998. Mode of action of linear amphipathic α-helical antimicrobial peptides. *Biopolymers (Peptide Sci.).* 47:451–463.

Riquelme, G., E. Lopez, L. M. Garcia-Segura, J. A. Ferragut, and J. M. Gonzalez-Ros. 1990. Giant liposomes: a model system in which to obtain patch-clamp recordings of ionic channels. *Biochemistry.* 29: 11215–11222.

Robinson, W. E., Jr., B. McDougall, D. Tran, and M. E. Selsted. 1998. Anti-HIV-1 activity of indolicidin, an antimicrobial peptide from neutrophils. *J. Leukocyte Biol.* 63:94–100.

Saberwal, G., and R. Nagaraj. 1994. Cell-lytic and antibacterial peptides that act by perturbing the barrier function of membranes: facets of their conformational features, structure-function correlations and membrane-perturbing abilities. *Biochim. Biophys. Acta.* 1197:109–131.

Sansom, M. S. 1991. The biophysics of peptide models of ion channels. *Prog. Biophys. Mol. Biol.* 55:139–235.

Schluesener, H. J., S. Radermacher, A. Melms, and S. Jung. 1993. Leukocytic antimicrobial peptides kill autoimmune T cells. *J. Neuroimmunol.* 47:199–202.

Schnorf, M., I. Potrykus, and G. Neuhaus. 1994. Microinjection technique: routine system for characterization of microcapillaries by bubble pressure measurement. *Exp. Cell Res.* 210:260–267.

Selsted, M. E., M. J. Novotny, W. L. Morris, Y. O. Tang, W. Smith, and J. S. Cullor. 1992. Indolicidin, a novel bactericidal tridecapeptide amide from neutrophils. *J. Biol. Chem.* 267:4292–4295.

Shai, Y. 1999. Mechanism of the binding, insertion, and destabilization of phospholipid bilayer membranes by α-helical antimicrobial and cell non-selective membrane-lytic peptides. *Biochim. Biophys. Acta.* 1462: 55–70.

Sitaram, N., and R. Nagaraj. 1999. Interaction of antimicrobial peptides with biological and model membranes: structural and charge requirements for activity. *Biochim. Biophys. Acta.* 1462:29–54.

Subbalakshmi, C., V. Krishnakumari, R. Nagaraj, and N. Sitaram. 1996. Requirements for antibacterial and hemolytic activities in the bovine neutrophil derived 13-residue peptide indolicidin. *FEBS Lett.* 395: 48–52.

Tytler, E. M., G. M. Anantharamaiah, D. E. Walker, V. K. Mishra, M. N. Palgunachari, and J. P. Segrest. 1995. Molecular basis for prokaryotic specificity of magainin-induced lysis. *Biochemistry.* 34:4393–4401.

van Ginkel, G., H. van Langen, and Y. K. Levine. 1989. The membrane fluidity concept revisited by polarized fluorescence spectroscopy on different model membranes containing unsaturated lipids and sterols. *Biochimie.* 71:23–32.

Verger, R., and F. Pattus. 1976. Spreading of membranes at the air/water interface. *Chem. Phys. Lipids.* 16:285–91.

Wieprecht, T., M. Dathe, M. Beyermann, E. Krause, W. L. Maloy, D. L. MacDonald, and M. Bienert. 1997. Peptide hydrophobicity controls the activity and selectivity of magainin 2 amide in interaction with membranes. *Biochemistry.* 36:6124–6132.

Williams, R. W., R. Starman, K. M. P. Taylor, T. Gable, T. Beeler, and M. Zasloff. 1990. Raman spectroscopy of synthetic antimicrobial frog peptides magainin 2a and PGLa. *Biochemistry.* 29:4490–4496.

Wimley, W. C., and S. H. White. 1996. Experimentally determined hydrophobicity scale for proteins at membrane interfaces. *Nat. Struct. Biol.* 3:842–848.

Wu, M., E. Maier, R. Benz, and R. E. W. Hancock. 1999. Mechanism of interaction of different classes of cationic antimicrobial peptides with planar bilayers and with the cytoplasmic membrane of *Escherichia coli. Biochemistry.* 38:7235–7242.

Zasloff, M. 1987. Magainins, a class of antimicrobial peptides from *Xenopus* skin: isolation, characterization of two active forms, and partial cDNA sequence of a precursor. *Proc. Natl. Acad. Sci. U.S.A.* 84: 5449–5453.

Zasloff, M., B. Martin, and H.-C. Chen. 1988. Antimicrobial activity of synthetic magainin peptides and several analogues. *Proc. Natl. Acad. Sci. U.S.A.* 85:910–913.